

¹⁰The current limits for production of charmed mesons by protons with their subsequent decay into final states with two charged particles are roughly equal to the production cross sections for ψ 's by 400-GeV protons

[E. Shibata, in Proceedings of the Second International Conference at Vanderbilt University on New Results in High Energy Physics, Nashville, Tennessee, 1-3 March 1976 (to be published)].

Charm Threshold in Electron-Positron Annihilation

Kenneth Lane*

Laboratory of Nuclear Studies, Cornell University, Ithaca, New York 14853

and

E. Eichten†

Institute for Advanced Study, Princeton, New Jersey 08540

(Received 11 June 1976)

Available data on new mesons discovered at SPEAR are sufficient to determine the spectrum of low-lying charmed mesons and to provide a complete description of the threshold structure of R in the framework of the charmonium model. A number of simple tests are proposed to confirm the charm interpretation.

Recent observation at SPEAR of the reaction $e^+e^- \rightarrow (K^{\mp}\pi^{\pm} \text{ or } K^{\mp}\pi^{\mp}\pi^{\pm}\pi^{\pm}) + (\text{recoil, strangeness } \pm 1)$ ¹ strongly suggests that the long-awaited charmed mesons have been found. The identified $K\pi$ and $K\pi\pi\pi$ systems appear as 6-7 standard deviation enhancements at 1.865 ± 0.010 GeV. A large signal is also observed in recoil against the 1.865 state for recoil invariant masses in the range 1.96 to 2.20 GeV. All of this comes from analysis of data taken in the "threshold region," $3.90 \text{ GeV} \leq W \leq 4.60 \text{ GeV}$, with little or no evidence for the enhancements at $W \approx 5-6$ GeV.

Choosing the mass of the state seen in recoil to be 2.02 GeV in accord with Ref. (1), these new data permit resolution of two important issues: (1) The charmed pseudoscalar D^0 lies at 1.865 GeV, below the vector D^{*0} at 2.02 GeV. (2) The rich structure in R observed between 3.7 and 4.5 GeV is completely consistent with the charmonium model, generalized to include coupling to decay channels. Furthermore, we can estimate masses of all other low-lying charmed mesons, the D^* branching ratios, and the exclusive channel contributions to ΔR , the charmed component of R . We propose a number of tests of this "charm interpretation" of the SPEAR results.

Systematics of charmed mesons.—As we argue shortly, $M_{D^0} = 1.865$ GeV and $M_{D^{*0}} \approx 2.020$ GeV. From the quark model, $M_{D^+} - M_{D^0} = M_{K^0} - M_{K^+}$ and $M_{F^+} - M_{D^0} = M_{\phi} - M_{K^*}$. Thus, $M_{D^+} = 1.870$ GeV, $M_{D^{*+}} = 2.025$ GeV, $M_{F^+} \approx 2.00$ GeV, and $M_{F^{*+}} \approx 2.15$ GeV. A linear-potential model calculation² places the center of gravity of the

charmed P states 550 MeV above the S states. Spin-dependent splittings among the P states can be taken from the strange-meson system (the reduced masses are reasonably close). The estimated P -state masses are $D_P(1^1P_1) \approx 2.5$ GeV, $D_{P_0}(1^3P_0) \approx 2.4$ GeV, $D_{P_1}(1^3P_1) \approx 2.6$ GeV, and $D_{P_2}(1^3P_2) \approx 2.6$ GeV.

These considerations set the following thresholds in e^+e^- annihilation below 4.5 GeV: $W_{DD} = 3.73$ GeV, $W_{DD^*} = 3.885$ GeV, $W_{FF} = 4.00$ GeV, $W_{D^*D^*} = 4.04$ GeV, $W_{FF^*} = 4.15$ GeV, $W_{F^*F^*} = 4.30$ GeV, $W_{DDP} \approx W_{D^*D_{P_0}} \approx 4.4$ GeV, and $W_{DD_{P_1}} \approx 4.5$ GeV.

There is no phase-space inhibition for the decay modes $D_P \rightarrow D^*\pi$, $D_{P_0} \rightarrow D\pi$, $D_{P_1} \rightarrow D^*\pi$, and $D_{P_2} \rightarrow D\pi, D^*\pi, F^+\bar{K}$.³ However, phase space for $D^* \rightarrow D\pi$ is limited, and $D^* \rightarrow D\gamma$ can be competitive. Note that $F^{*+} \rightarrow F^+\gamma$ is the only observable mode of the $C=S=1$ vector. These are sensitive to all relevant mass differences. We computed $\Gamma(D^* \rightarrow D\pi)$ by two quite different methods: (i) calculation of the amplitude using the model of Eichten *et al.*⁴; (ii) assuming SU(4) symmetry and relating to $\Gamma(K^* \rightarrow K\pi)$. Good agreement between the two methods establishes insensitivity to dynamical details. Radiative ($M1$) transitions are computed from the nonrelativistic quark model.^{2,5} Results are listed in Table I.

Charmed-meson production in e^+e^- annihilation.—Recently we presented a dynamical model for $e^+e^- \rightarrow$ charmed mesons,⁴ based on a universal interaction (linear potential) responsible for both quark binding and hadronic decay. The annihila-

TABLE I. Final-particle momenta, decay rates, and branching ratios for D^* decays, calculated with the model of Ref. 4. Branching fractions obtained from the SU(4) assumption are 0.66, 0.31, and 0.03 for D^{*+} ; 0.27, 0.36, and 0.37 for D^{*0} . $\Gamma(F^{*+} \rightarrow F^+\gamma) = 1.6$ keV.

Decay	Momentum (MeV)	Rate (keV)	Branching Ratio
$D^{*+} \rightarrow D^0\pi^+$	75	182	0.67
$\rightarrow D^+\pi^0$	73	84	0.31
$\rightarrow D^+\gamma$	149	4.5	0.02
$D^{*0} \rightarrow D^+\pi^-$	53	64	0.32
$\rightarrow D^0\pi^0$	73	84	0.42
$\rightarrow D^0\gamma$	149	54	0.27

tion cross section is the absorptive part of $\sum_{n,m}(e^+e^- \rightarrow \psi_n \rightarrow \text{charm-meson pair} \rightarrow \psi_m \rightarrow e^+e^-)$, with ψ_n a 3S_1 or 3D_1 charmonium level.

General features of this model relevant here are the following: (1) The basic charmed-meson production process is a *sequential* two-body one. For example, $e^+e^- \rightarrow D^*\bar{D}^* \rightarrow (D\pi) + (\bar{D}\pi)$.⁶ (2) The $\psi_n \rightarrow D\bar{D}$ form factor falls rapidly with increasing D momentum. Thus, any exclusive channel is important only for energies near its threshold. (3) $\sigma_D \equiv \sigma(e^+e^- \rightarrow D^+D^-) = \sigma(e^+e^- \rightarrow D^0\bar{D}^0)$, and similarly for $\sigma_{DD^*} = \sigma(e^+e^- \rightarrow D^{*+}D^-)$ and $\sigma_{D^*} = \sigma(e^+e^- \rightarrow D^{*+}D^{*-})$. (4) For $M_D = M_{D^*}$, $\sigma_D : \sigma_{DD^*} : \sigma_{D^*} = 1:2:[7+6(P_{D^*}/M_{D^*})^2 + (P_{D^*}/M_{D^*})^4]$. This relation holds reasonably well for unequal masses above $W_{D^*D^*}$. The strongest peak in recoil against D or D^* is the \bar{D}^* (for $W \lesssim 4.4-4.5$ GeV), which implies $M_{D^*0} = 2.02$ GeV while $M_{D^0} = 1.865$ GeV. (5) The rate for $\psi_n(c\bar{c}) \rightarrow (c\bar{q}) + (\bar{c}q)$ decreases as m_q^{-4} for $m_c \gg m_q \sim 0.2-0.6$ GeV. Thus F production is a negligible contribution to ΔR in

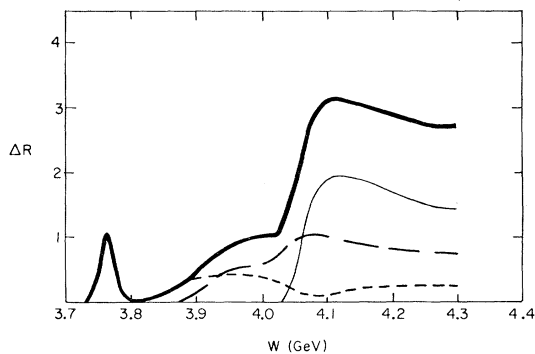


FIG. 1. Charm component ΔR (heavy solid line) for $W \leq 4.3$ GeV, and its dominant exclusive contributions: R_D (short-dashed), R_{DD^*} (long-dashed), and R_{D^*} (light solid). Parameters for this model calculation are given in Ref. 4.

the threshold region. Using the D and D^* masses given above and the bare quark parameters of Ref. 4, we have computed the exclusive cross section ratios $R_D = 2\sigma_D/\sigma_\mu$, $R_{DD^*} = 4\sigma_{DD^*}/\sigma_\mu$, and $R_{D^*} = 2\sigma_{D^*}/\sigma_\mu$. The results are shown in Fig. 1, along with their approximate sum ΔR . Since charmed P states were not included we restrict our calculations to $W_{DD} \leq W \leq 4.3$ GeV and we cannot expect exact agreement between ΔR and experiment. However, the structure of the exclusive channels should be a reliable guide to the data.

We now interpret the observed structure⁷ of R (Fig. 2) in terms of charm production, suggesting several tests which require only moderate statistics. We use our computations of exclusive-channel contributions to R , together with the estimated D^* branching ratios, to indicate the *expected* outcome of these tests.

The invariant mass M_x recoiling against D^0 and D^+ reveals much about the spectrum of charmed mesons as well as details of various exclusive channels (branching fractions, e.g.). M_x will show strong energy dependence in the threshold region and maximum signal-to-background ratio requires *separate* analysis of data from several subregions. We discuss each one in turn.

$3.73 \text{ GeV} \leq W \leq 3.88 \text{ GeV}$.—Clean isolation of the lowest charmed mesons, uncontaminated by γ 's and π 's from D^* and D_P decays, is possible only in this region. The *only* significant $D\bar{D}$ signal is at the peak of the 3D_1 charmonium level, seen in Fig. 1 at 3.77 GeV. Two 2-standard-deviation bumps ($\Delta R \sim 1.5$) of similar shape, at 3.77 and 3.84 GeV, have been reported.^{7,8} Additional running over this region is required to confirm either a 3D_1 . We emphasize that fully 25–40% of all e^+e^- reactions at the peak will yield a pure $D\bar{D}$ final state.

Discovery of D^+ is crucial, and makes it com-

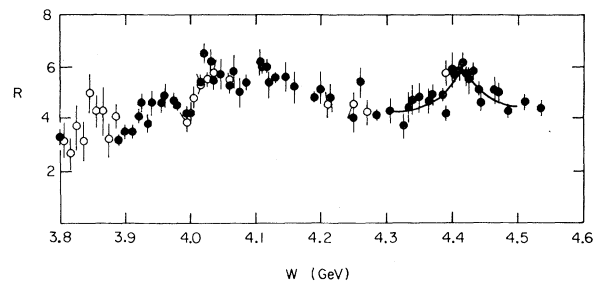


FIG. 2. Data for R (Ref. 7). Closed and open circles represent data from runs separated in time by several months.

elling to determine the 1^3D_1 peak, where its production constitutes half of ΔR . An important test of the charm⁹ and sextet-enhancement selection rules¹⁰ is that the only probable (D^+ → all charged) transitions are $K^-\pi^+\pi^+$ and $K_S\pi^-\pi^+\pi^+$. Finally, a search for single leptons in the recoil against D measures directly its inclusive semileptonic-nonleptonic branching ratio and, possibly, tests the $\Delta C = \Delta S$ rule.

$3.88 \text{ GeV} \leq W \leq 4.04 \text{ GeV}$.—Opening of DD^* at 3.88 GeV in Fig. 1 agrees well with the rise observed in the data between 3.90 and 3.97 GeV. The subsequent falloff, from 3.97 to 4.00 GeV in Fig. 2, is due to $\psi_n - D\bar{D}$ form-factor effects. There next appears in Fig. 2 a sharp rise of $\Delta R \approx 3$ at $W = 4.01\text{--}4.03 \text{ GeV}$. Since the $D^*\bar{D}^*$ channel is not yet open, this must be interpreted as the 3^3S_1 level. The mass, therefore, is 4.03 GeV.¹¹

In addition to $M_x = M_D$, two new effects leading to overlapping enhancements in M_x now appear. The obvious one is $M_x = M_{D^*} = 2.02 \text{ GeV}$. The second is a kinematic enhancement corresponding to observation of D in $e^+e^- \rightarrow D^*\bar{D} \rightarrow D(\pi\bar{D})$, and is a consequence of the small pion momentum. For $p_\pi = 75 \text{ MeV}$ in the D^* rest frame, $M_x = M_{\bar{D}\pi}$ lies in the range 2.01 to 2.03 GeV (for $W = 3.90 \text{ GeV}$), 2.00 to 2.06 GeV ($W = 3.95 \text{ GeV}$), and 2.00 to 2.09 GeV ($W = 4.05 \text{ GeV}$). Data taken over this region will show a pileup at $M_x = 2.00\text{--}2.01 \text{ GeV}$.¹² The frequency of events in which $\bar{D} + \pi$ recoils against D relative to those in which \bar{D}^* does is $B_{\pi^0} + B_{\pi^+} \approx 1.1$ if D^0 is observed, and $B_{\pi^-} + B_{\pi^0} \approx 0.6$ if D^+ is. [Our notation is $B_{\pi^-} = \Gamma(D^{*0} \rightarrow \pi^- D^+)/\Gamma(D^{*0})$, etc.] Once D^* production becomes important,

there will be a substantial increase in the fraction of slow pions, $p_\pi^{\text{lab}} \lesssim 100\text{--}150 \text{ MeV}$ and $x = p_\pi^{\text{lab}}/W \lesssim 0.04$.¹³

$4.04 \text{ GeV} \leq W \leq 4.35 \text{ GeV}$.—The model calculation shows that $D^*\bar{D}^*$ production, influenced by the nearby 3^3S_1 pole, contributes a large and rapid rise to R . When compared with the rise beginning at $\sim 4.05 \text{ GeV}$ in Fig. 2, it is clear that the points from there to 4.3 GeV represent the opening and subsequent decay of this channel. The absence of further clear thresholds in this region is consistent with the quark-mass suppression of F and F^* production mentioned above. The $\bar{D}D_p$ channel, expected to have a strong S -wave threshold, presumably does not open below $\sim 4.4 \text{ GeV}$.

A new kinematic enhancement appears at 2.16 GeV corresponding to $\bar{D}^* + \pi$ recoiling against D . For $p_\pi = 75 \text{ MeV}$ in the D^* rest frame, $2.16 \text{ GeV} \leq M_x \leq 2.21 \text{ GeV}$ at $W = 4.10 \text{ GeV}$, and $2.16 \text{ GeV} \leq M_x \leq 2.27 \text{ GeV}$ at $W = 4.30 \text{ GeV}$. For $p_\pi = 50 \text{ MeV}$, the allowed ranges are 2.16 to 2.19 GeV ($W = 4.10 \text{ GeV}$) and 2.17 to 2.24 GeV ($W = 4.30 \text{ GeV}$). $\bar{D}^* + \gamma$ recoiling against D has a much broader M_x distribution ($2.12 \text{ GeV} \leq M_{\bar{D}^*\gamma} \leq 2.22 \text{ GeV}$ at $W = 4.1 \text{ GeV}$) and does not accumulate at any particular energy for data taken over this region.

Measuring the relative strengths of various enhancements not only tests our interpretation of the data, but proves useful in extracting branching ratios and exclusive cross sections. We mention two examples.

(1) The ratio of events with $\bar{D}^* + \pi$ recoiling against D to those with \bar{D}^* in recoil is

$$N(\bar{D}^*\pi \text{ against } D^0)/N(\bar{D}^* \text{ against } D^0) = 2(B_{\pi^0} + B_{\pi^+})R_{D^*}/R_{DD^*}, \quad (1)$$

A similar expression holds for D^+ . Integrating over this region, we find that the relative strength of the two enhancements opposite D^0 is $\sim 3.7:1$. The integrated ratio for recoil against D^+ is $\sim 2.1:1$. Although the $\bar{D}\pi$ kinematic effect is now quite broad, it may still confuse identification of true \bar{D}^* . For example, at $W = 4.25 \text{ GeV}$, $2.01 \text{ GeV} \leq M_{\bar{D}\pi} \leq 2.14 \text{ GeV}$ (for $p_\pi = 75 \text{ MeV}$) and $2.02 \text{ GeV} \leq M_{\bar{D}\pi} \leq 2.11 \text{ GeV}$ (for $p_\pi = 50 \text{ MeV}$). Data taken over this entire region will show an accumulation at $M_x = 2.00\text{--}2.02 \text{ GeV}$.

(2) If D^0 is observed through its decay mode f , then D^{*+} should be seen in $f\pi^+$. The expected relative frequencies are

$$\rho_+ \equiv N(D^{*+} \rightarrow \pi^+ f)/N(D^0 \rightarrow f) = B_{\pi^+}(R_{DD^*}/2 + R_{D^*})/[R_D + R_{DD^*}/2 + (B_{\pi^+} + B_{\pi^0} + B_\gamma)(R_{DD^*}/2 + R_{D^*})]. \quad (2)$$

A similar formula gives $\rho_0 = N(D^{*0} \rightarrow \pi^0 f)/N(D^+ \rightarrow f)$.

Onset and decay of various thresholds give ρ_+ and ρ_0 strong energy dependence. We find $\rho_+ \approx 0.1$ to 0.2 for $3.9 \text{ GeV} \lesssim W \lesssim 4.04 \text{ GeV}$, followed by a sharp rise to 0.4, maintained from 4.04 to 4.35 GeV. Integrated over 3.88–4.35 GeV, the ratio of ($D^{*+} \rightarrow \pi^+ f$) to ($D^0 \rightarrow f$) events is ≈ 0.37 .

ρ_0 jumps from 0.1 below 4.04 GeV to 0.33 above; the integrated ratio of ($D^{*0} \rightarrow \pi^0 f$) to ($D^+ \rightarrow f$) events is 0.30.

$4.35 \text{ GeV} \leq W \leq 4.60 \text{ GeV}$.—Assignment of 3^3S_1 at 4.03 GeV forces our reinterpretation⁴ of the 4.4-GeV structure¹⁴ (Fig. 2) as the 4^3S_1 level:

(i) $4.41 - 4.03 \approx 0.4$ GeV is consistent with the charmonium separation $M(4^3S_1) - M(3^3S_1)$, not with $M(4^3S_1) - M(2^3D_1)$. (ii) $\Gamma_e(4.4) \approx 0.4$ keV implies $|\psi_{4,4}(0)|/|\psi_{3,1}(0)| \approx 0.4$, too large for a 3D_1 state.¹⁵ Beware that nonrelativistic level designation may be meaningless by now. The important test that this is a charmonium level is a sharp increase in D production at $\psi(4.4)$.

Charmed P states, if not very broad, will show in recoil against D, D^* at these higher energies. Further signals are these: (i) There are sudden jumps in ρ_+ and ρ_0 (generalized to include these new channels). (ii) The slow-pion effect diminishes as the $D^*\bar{D}^*$ channel does, until $W \gtrsim W_{D^*D_P}$, $W_{D^*D_{P0}}$ when slow D^* 's are produced once again. (iii) A search for \bar{D}_P opposite D at $\psi(4.4)$ is worthwhile.

The foregoing considerations demonstrate that much remains to be done at SPEAR to determine the nature of the new quantum number and map out the newest spectroscopy.

*Work supported in part by the National Science Foundation.

†Work supported in part by the U. S. Energy Research and Development Administration Grant No. E(11-1)-2220.

¹G. Goldhaber *et al.*, Phys. Rev. Lett. **37**, 255 (1976).

²E. Eichten *et al.*, Phys. Rev. Lett. **34**, 369 (1975).

For this pure linear potential ($V = r/a^2$) calculation, the parameters are $m_c = 1.836$ GeV, $a = 1.944$ GeV⁻¹; also, the light-quark masses are taken to be $m_u = m_d = 0.30$ GeV, $m_s = 0.40$ GeV.

³We assume that P -state widths are not so great as to wash out their threshold effects. If SU(4) symmetry may be used to determine their widths from those of the strange P states, we get $\Gamma(D_P) \approx \Gamma(D_{P0}) \approx 90$ MeV, $\Gamma(D_{P1}) \approx 75$ MeV, and $\Gamma(D_{P2}) \approx 30$ MeV.

⁴E. Eichten *et al.*, Phys. Rev. Lett. **36**, 500 (1976).

The *bare* charmed-quark mass and linear-potential strength used for the present coupled-channel computations are the same as in this reference: $m_c^0 = 1.910$ GeV, $a^0 = 1.582$ (GeV)⁻¹; $m_u = m_d = 0.31$ GeV, $m_s = 0.40$ GeV. The unrenormalized masses of the 3^3S_1 , 4^3S_1 , and 2^3D_1 states have been artificially lowered by 50

MeV in a crude attempt to mock the effects of charmed P states, not included in our model.

⁵R. Van Royen and V. F. Weisskopf, Nuovo Cimento **50**, 617 (1967).

⁶The essentially treelike structure of hadronic processes is discussed by K. Lane and S. Rudaz (to be published), who emphasize its utility for meson spectroscopy in the final states of ψ -family decays. See also S. Rudaz, Phys. Rev. D **11**, 1915 (1975), and references therein.

⁷Stanford Linear Accelerator Center-Lawrence Berkeley Laboratory collaboration, as reported by H. Lynch, in Proceedings of the International Conference on the Production of Particles with New Quantum Numbers, Madison, Wisconsin, April 22-24, 1976 (to be published).

⁸The bump at 3.77 GeV, not shown in Fig. 2, consists of two data points, separated by ~ 10 MeV, each 2 standard deviations above background.

⁹S. Glashow, J. Iliopoulos, and L. Maiani, Phys. Rev. D **2**, 1285 (1970); J. D. Bjorken and S. L. Glashow, Phys. Lett. **11**, 255 (1964).

¹⁰M. Einhorn and C. Quigg, Phys. Rev. D **12**, 2015 (1975), and references therein. Decays leading to $K^-\pi^+\pi^+$ are $D^+ \rightarrow \pi^+\bar{K}^{*0}$, $D^+ \rightarrow \pi^+\bar{K}^0(1300)$, while $D^+ \rightarrow \pi^+ + \bar{K}^0(1400) \rightarrow \pi^+ K_S^0 \pi^+\pi^-$. If sextet enhancement is correct, D^+ has considerably fewer Cabibbo-favored non-leptonic decay modes than does D^0 . Consequently, these modes have appreciable branching fractions. We estimate the ratio of events with D^+ to those with D^0 to be 1.0 for 3.73 GeV $\leq W \leq 3.88$ GeV, ≈ 0.75 at $W = 4.03$ GeV, and ≈ 0.62 for data uniformly taken between 3.73 and 4.30 GeV. It will be difficult to explain a D^+ signal much weaker than D^0 .

¹¹That the 3^3S_1 appears at 4.10 GeV, not 4.03 GeV, in our model calculations is almost certainly due to the neglect of higher thresholds, notably those involving D_P and D_{PJ} .

¹²Kinematic enhancements due to $\bar{D} + \gamma$ recoiling against D can further confuse identification of true \bar{D}^* , especially in the region 3.88 GeV $\leq W \leq 4.10$ GeV. We got 1.97 GeV $\leq M_{\bar{D}\gamma} \leq 2.07$ GeV ($W = 3.95$ GeV); 1.95 GeV $\leq M_{\bar{D}\gamma} \leq 2.12$ GeV ($W = 4.05$ GeV); and 1.94 GeV $\leq M_{\bar{D}\gamma} \leq 2.14$ GeV ($W = 4.10$ GeV).

¹³S. Nussinov, Phys. Rev. Lett. **35**, 1672 (1975).

¹⁴J. Siegrist *et al.*, Phys. Rev. Lett. **36**, 700 (1976).

¹⁵R. Barbieri *et al.*, CERN Report No. TH 2036, 1975 (unpublished); J. Pumplin, W. Repko, and A. Sato, Phys. Rev. Lett. **35**, 1538 (1975); H. J. Schnitzer, Phys. Rev. Lett. **35**, 1540 (1975).